Water-Assisted Alkaline Hydrolysis of Monobactams: A Theoretical Study

Natalia Díaz,[a] Dimas Suárez,[a] Tomás L. Sordo,*[a] Iñaki Tuñón,[b] and Estanislao Silla[b]

Abstract: A theoretical study of the water-assisted alkaline hydrolysis of 2-azetidinone, 3-formylamino-2-azetidinone and 3-formylamino-2-azetidine-1-sulfonate ion is carried out at the B3LYP/6-31+G* level. The effect of bulk solvent is taken into account using the PCM solvation model while specific solvent effects are represented by the inclusion of an ancillary water molecule along the reaction profile. The calculated free energy barriers in solution are in reasonable agreement with experimental values. The observed substituent effects due to the presence of the 3-formylamino and the SO_3 groups attached to the β-lactam ring are crucial factors determining the hydrolysis of monobactam antibiotics.

Keywords: alkaline hydrolysis · density functional calculations · monobactams · solvent effects · substituent effects

Introduction

It is generally accepted that β-lactam antibiotics kill bacteria by preventing the complete synthesis of the bacterial cell wall, thus leading to a defective bacterial cell wall which will rupture given the high internal cell pressure. This is accomplished by the acylation reaction between the antibiotic and the active site serine residue of transpeptidase enzymes (PBPs) which catalyze the cross-linking of the peptidoglycan chains as the main component of the bacterial cell wall.[1] The resultant acyl-enzyme intermediates are relatively stable, thus inhibiting the bacterial enzyme. However, β-lactamase enzymes, which are the primary means of resistance of pathogenic bacteria against β-lactam antibiotics, catalyze the hydrolysis of the antibiotic yielding biologically inactive products.[2–4]

Monobactams are monocyclic bacterially produced β-lactam antibiotics.[5, 6] They are characterized by the 3-formylamino-2-azetidine-1-sulfonic acid moiety. It has been suggested that the SO_3 group plays two essential roles.[7] Firstly, electron withdrawal which could activate the β-lactam amidic bond as does geometrical constraint in bicyclic β-lactams. Secondly, the positioning of the negative charge in monobactams, which is crucial for the biochemical activity of these drugs, is thought to be similar to that in penicillins and cephalosporins, in which it is located on the carboxylate group. Nevertheless, monobactams present particular characteristics in their mode of action and activity compared with that of bicyclic antibiotics. Thus, the antibacterial spectrum of monobactams is limited to aerobic Gram-negative bacteria, thus lacking affinity for the essential penicillin-binding proteins of Gram-positive bacteria and anaerobic organisms.[9] An important advantage of monobactams is that these compounds in general show a high degree of stability to the hydrolytic action of β-lactamases although some β-lactamases from *Klebsiella* and *Pseudomonas aureginosa* organisms have resulted in resistance against aztreonam, the first synthetic monobactam antibiotic drug.[9] Most interestingly, metallo-β-lactamases, in which the nucleophile is an hydroxyl group bound to a zinc ion, manifest a relatively low activity against these monocyclic antibiotics.[10] On the other hand, bridged monobactams across the C3–C4 bond have been reported as potent mechanism-based inhibitors of class C β-lactamases.[10]

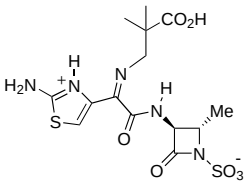

aztreonam

To further understand the biochemical activity of the β-lactam antibiotics, the alkaline hydrolysis of numerous β-lactam compounds has been studied extensively.[11] In an

[a] Dr. T. L. Sordo, Dr. N. Díaz, Dr. D. Suárez
Departamento de Química Física y Analítica
Universidad de Oviedo
C/ Julian Clavería 8, 33006, Oviedo Asturias (Spain)
Fax: (+34) 985 10 31 25
E-mail: tsordo@correo.uniovi.es

[b] Dr. I. Tuñón, Dr. E. Silla
Departamento de Química Física
Universidad de Valencia
46100, Burjassot, Valencia (Spain)

Supporting information for this article is available on the WWW under http://www.wiley-vch.de/home/chemistry/ or from the author. Cartesian coordinates for all the critical structures optimized at the B3LYP/6-31+G level. Figure showing the geometry and relative energies of the transition state for the addition of the $OH^- \cdots (H_2O)$ complex to 6-formylamino-3α-carboxypenam.

  0947-6539/02/0804-0859 $ 17.50+.50/0

experimental study of the alkaline hydrolysis of a series of monocyclic and bicyclic β-lactams,[12] it has been found that the rate-determining step for those processes corresponds to the addition of the hydroxide ion with $\Delta G^{\neq}$ values ranging from 18.2 to 25.4 kcal mol^{-1}. In the case of aztreonam, its reactivity towards alkaline hydrolysis is similar (within a factor of two) to that of benzylpenicillin.[14] It has been also found that the Arrhenius activation energy for its degradation in alkaline aqueous solution is 22.4 kcal mol^{-1} at pH 8.6.[13] On the other hand, it has been also reported that β-lactams of the more basic amines (e.g., nocardicin) present a positive deviation from the Brønsted plot of the second-order rate constants for the alkaline hydrolysis against the pK_a of the amine leaving group that may signify a change in rate-determining step to a breakdown of the tetrahedral intermediate.[14, 15]

Various factors have been proposed to explain the remarkable susceptibility of β-lactam antibiotics towards nucleophilic reagents,[16] namely, the relief of the β-lactam ring strain, the reduced amide resonance due to the lack of planarity of the β-lactam ring, the additional strain resulting from fusion with thiazolidine or dihydrothiazine rings, the influence of the acylamino side chain. For the alkaline hydrolysis reaction, β-lactams of basic amines show very similar reactivity to that of analogous non-cyclic amides whereas β-lactams of weakly basic amines, such as penicillin and cephalosporin antibiotics, show enhanced reactivity.[11] A comparative analysis of the reactivity of benzylpenicillin and related model compounds, has revealed that the increased reactivity of the penicillin β-lactam ring with respect to that of unsubstituted β-lactams, arises solely from the direct action of the fused ring structure and the acylamino side chain. The effect of the 3-acylamino group has been estimated as 2.1 kcal mol^{-1} at 30 °C.[12] In the case of monobactam antibiotics a similar effect of the 3-acylamino group is reasonably expected to determine together with the sulfonate functionality their inherent reactivity.

Theoretical work has been previously devoted to the investigation of the hydrolysis of β-lactams since the knowledge of the molecular mechanism of this process could be of great importance in the development of new antibacterial drugs and β-lactamase inhibitors.[16–23] In a theoretical study of the water-assisted alkaline hydrolysis of *N*-methylazetidinone, two different mechanisms were investigated.[22b] In both reaction paths, the first step corresponds to the nucleophilic attack of the hydroxyl anion solvated with a water molecule to the β-lactam carbonyl group to form a tetrahedral intermediate. An activation energy exists for this first step owing to the hydroxyl desolvation process modeled in a first approximation by the transfer of OH^- from the initial $OH^- \cdots (H_2O)$ complex to the β-lactam molecule. The two mechanisms evolve from different conformers of the tetrahedral complex through asynchronous ring opening and proton transfer to the negatively charged nitrogen atom to give the final product.

In this paper we report a quantum chemical study of the alkaline hydrolysis of the following model compounds: 2-azetidinone (**AZ**), 3-formylamino-2-azetidinone (**FAZ**), and 3-formylamino-2-azetidine-1-sulfonate ion (**FAZS**). For **FAZ** and **FAZS** we investigated both possibilities for the nucleophilic attack, *syn* or *anti* with respect to the formylamino side chain. The conformation of this formylamino side chain has been chosen in agreement with the available X-ray structure for aztreonam.[24] The comparative study of these model compounds will allow us to obtain a deeper understanding of the mechanism of action of monobactams and the role played by the formylamino side chain and the characteristic SO_3 group. The effect of bulk solvent is taken into account using a continuum model while specific solvent effects are represented by including an ancillary water molecule which can act as both proton donor and proton acceptor participating in the definition of the reaction coordinate. By directly addressing the theoretical results with the experimental data on the alkaline hydrolysis of monobactams, we discuss how this reaction is controlled through a balance between substituent and solvent effects.

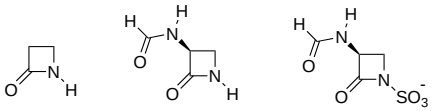

Computational Methods

Calculations were carried out with the *Gaussian 98* system of programs.[25] Stable structures were fully optimized and transition structures (TS) located at the B3LYP/6-31+G* level. All the critical points were further characterized by analytic computation of harmonic frequencies at the same theory level. Thermodynamic data (298 K, 1 bar) were computed using the B3LYP/6-31+G* frequencies within the ideal gas, rigid rotor, and harmonic oscillator approximations.[26] $\Delta G_{\text{gas phase}}$ energies were obtained for all of the optimized species by combining the B3LYP/6-31+G* electronic energies with the zero-point vibrational energy (ZPVE) values and thermal corrections.

Quantum chemical computations in solution were carried out on gas phase optimized geometries using a general self consistent reaction field (SCRF) model.[27] In this model, the solvent is represented by a dielectric continuum characterized by its relative static dielectric permittivity, ε. The solute is placed in a cavity created in the continuum, the shape of which is chosen to fit as best as possible the solute molecular shape according to the solvent excluding surface.[28] The solute charge distribution polarizes the dielectric which in turn creates an electric field that modifies the charge distribution of the solute. One may take into account this interaction by minimizing the energy of the solute plus the electrostatic free energy change corresponding to the solvation process that is given by

$$\Delta G_{\text{solvation}} = -\tfrac{1}{2} E_{\text{int}}$$

where E_{int} is the interaction energy:

$$E_{\text{int}} = \sum_{\alpha} V_{\text{el}}(\boldsymbol{r}_\alpha) Z_\alpha - \int V_{\text{el}}(\boldsymbol{r}) \rho(\boldsymbol{r}) \, \mathrm{d}\boldsymbol{r}$$

In this equation, V_{el} is the electrostatic potential created by the polarized continuum in the cavity, $\boldsymbol{r}_\alpha$ and Z_α are the position vector and the charge of nucleus α, respectively, and $\rho(\boldsymbol{r})$ is the electronic density at point $\boldsymbol{r}$. The factor ½ in the free energy arises from the fact that the positive work required to polarize the medium is exactly one-half the value of the interaction energy. V_{el} may be computed following different approaches. The recently derived UAHF (united atom Hartree–Fock) parametrization[29] of the polarizable continuum model (PCM)[27c] was used, including both electrostatic and non-electrostatic solute–solvent interactions.[30] The topology of the system was controlled so that the hybridization of all the atoms was the same in analogous structures. A relative permittivity of 78.39 was used to simulate water as solvent.

0947-6539/02/0804-0860 $ 17.50+.50/0 *Chem. Eur. J.* **2002**, *8*, No. 4

Addition of $\Delta G_{\text{gas phase}}$ to the corresponding relative solvation Gibbs energies, $\Delta\Delta G_{\text{solvation}}$, evaluated neglecting the change in the relative value of the thermal corrections when going from a vacuum to the solution, gives $\Delta G_{\text{solution}}$ for the structures studied in this work.

Atomic charges were computed in the gas phase carrying out a natural population analysis (NPA) using the corresponding B3LYP/6-31+G* density matrices.[31]

Results and Discussion

In the present work, we investigated the mechanism for the alkaline hydrolysis of 2-azetidinone (**AZ**), 3-formylamino-2-azetidinone (**FAZ**) and 3-formylamino-2-azetidine-1-sulfonate ion (**FAZS**) in which the hydrogen transfer is mediated by a water molecule. This route has been previously seen to be the most favored one for the alkaline hydrolysis of azetidinones.[22b] As previously mentioned, both *syn* and *anti* mechanisms were studied for **FAZ** and **FAZS**. First we present the results obtained for the hydrolysis of 2-azetidinone and 3-formylamino-2-azetidinone which have the same mechanism, and then those for the hydrolysis of 3-formylamino-2-azetidine-1-sulfonate ion. Unless otherwise stated the electronic energy including the ZPVE correction will be given in the text.

Hydrolysis of 2-azetidinone and 3-formylamino-2-azetidinone: Figures 1 and 2 present the stationary structures located for the alkaline hydrolysis of 2-azetidinone and the *syn* and *anti* routes of 3-formylamino-2-azetidinone, respectively. Tables 1 and 2 display the corresponding relative energies with respect to the $OH^- \cdots (H_2O)$ complex and the β-lactam compound.

Min$_1$(AZ) and **Min$_1$(FAZ)-*syn*** in Figure 1 and 2 are critical structures corresponding to reactant complexes formed through interaction of the hydroxyl anion solvated by one water molecule with 2-azetidinone and 3-formylamino-2-azetidinone, respectively. In **Min$_1$(AZ)** the hydroxyl oxygen atom is situated at 1.417 Å from the hydrogen atom of the solvating water molecule and at 2.022 Å from the hydrogen atom of the C3 methylene group while the oxygen atom of the water molecule is interacting with the hydrogen atom of the C4 methylene group at a distance of 2.266 Å, leading to a stabilization of 14.3 kcal mol^{-1} relative to separate reactants. In the **Min$_1$(FAZ)-*syn*** structure, the oxygen atom of the hydroxyl anion is strongly interacting with the NH of the β-lactam side chain at a distance of 1.477 Å. This short hydrogen bond between the 3-formylamino group and the attacking hydroxyl moiety greatly stabilizes **Min$_1$(FAZ)-*syn*** which is 35 kcal mol^{-1} below separate reactants. For the *anti* attack of the $OH^- \cdots (H_2O)$ dimer towards the β-lactam carbonyl of **FAZ**, geometry optimizations in the gas phase as well as IRC calculations started from the **TS$_1$(FAZ)-*anti*** structure, gave an initial complex for the *anti* process in which the hydroxyl anion abstracts a proton from the formylamino group of **FAZ**. This structure is not reported since it is not relevant for the actual reaction in aqueous solution.

According to our calculations, **TS$_1$(AZ)**, **TS$_1$(FAZ)-*syn***, and **TS$_1$(FAZ)-*anti*** are transition states corresponding to the nucleophilic attack of the hydroxyl anion on the carbonylic C atom of the β-lactam. This nucleophilic attack involves the partial desolvation of the hydroxyl anion, a slight breaking of the C–N amide bond, and the partial formation of the C–O bond with a distance of 2.281, 2.023, and 2.339 Å at **TS$_1$(AZ)**, **TS$_1$(FAZ)-*syn***, and **TS$_1$(FAZ)-*anti***, respectively (see Figures 1 and 2). In the gas phase, the energies of these TSs with respect to the β-lactam compound and the $OH^- \cdots (H_2O)$ dimer are -0.7, -19.8, and -14.8 kcal mol^{-1} for **TS$_1$(AZ)**, **TS$_1$(FAZ)-*syn***, and **TS$_1$(FAZ)-*anti***, respectively. **TS$_1$(AZ)**, **TS$_1$(FAZ)-*syn*** are 15.0 and 15.2 kcal mol^{-1} less stable than their precursors on the PES, **Min$_1$(AZ)** and **Min$_1$(FAZ)-*syn***, respectively. Among these TSs, **TS$_1$(FAZ)-*syn*** results the most stable and the most advanced transition state for nucleophilic attack due to the presence of a hydrogen-bond interaction between the formylamino side chain and the attacking hydroxyl anion with a short N-H$\cdots$O distance of 1.777 Å. Note that the small size of the hydroxyl anion makes the *syn* pathway sterically feasible. On the other hand, with respect to the non-substituted **TS$_1$(AZ)** structure, the *anti* pathway for **FAZ** proceeds through an earlier transition state given that the electron-withdrawing effect of the formylamino side chain makes the β-lactam carbonyl group a better electrophile. The position of the ancillary water depends on the "reactant-like" character of the TSs. Thus, the water molecule bridges the nucleophile and the endocyclic N atom of β-lactam in the advanced TSs (**TS$_1$(AZ)** and **TS$_1$(FAZ)-*syn***) where it merely solvates the nucleophile in the less advanced one (**TS$_1$(FAZ)-*anti***).

The addition products, **Min$_2$(AZ)**, **Min$_2$(FAZ)-*syn***, and **Min$_2$(FAZ)-*anti***, correspond to tetrahedral intermediates interacting with the ancillary water molecule by means of one (**Min$_2$(FAZ)-*anti***) or two (**Min$_2$(AZ)** and **Min$_2$(FAZ)-*syn***) hydrogen bonds. These tetrahedral intermediates can achieve different conformations depending on the *syn*/*anti* relationship between the nitrogen lone pair and the hydroxyl group as well as on the orientation of the hydroxyl hydrogen. Several pathways, not detailed here, would be feasible for connecting the **Min$_2$(AZ)**, **Min$_2$(FAZ)-*syn***, and **Min$_2$(FAZ)-*anti*** structures with the **Min$_3$(AZ)**, **Min$_3$(FAZ)-*syn***, and **Min$_3$(FAZ)-*anti*** intermediates passing through low barrier steps (i.e., internal rotations, pyramidal inversion of the N atom, relocation of the ancillary water molecule, etc.). The **Min$_3$(AZ)**, **Min$_3$(FAZ)-*syn***, and **Min$_3$(FAZ)-*anti*** structures are more stable than reactants by 5.2, 14.9, and 22.4 kcal mol^{-1}, respectively. The greater stability of **Min$_3$(FAZ)-*anti*** results most likely from the N-H$\cdots$O hydrogen bond formed between the 3-formylamino side chain and the negatively charged carbonylic O atom.

In **Min$_3$(AZ)**, **Min$_3$(FAZ)-*syn***, and **Min$_3$(FAZ)-*anti***, the relative orientation of the water molecule and the hydroxyl moiety is suitable for double proton exchange.[22b] We found that these structures evolve readily through a single transition structure to give the ring opening and proton transfer from the hydroxyl group to water and from that to the nitrogen atom. The corresponding TSs, **TS$_2$(AZ)**, **TS$_2$(FAZ)-*syn***, and **TS$_2$(FAZ)-*anti***, present very low electronic energy barriers of 1.1, 0.3, and 4.3 kcal mol^{-1} with respect to **Min$_3$(AZ)**, **Min$_3$(FAZ)-*syn***, and **Min$_3$(FAZ)-*anti***, respectively (0.4, -0.6,

and 3.6 kcal mol^{-1} when the ZPVE is taken into account). In the final product conformers **P(AZ)**, **P(FAZ)-*syn***, and **P(FAZ)-*anti***, the formed carboxylate and the leaving amino group are interacting through the ancillary water molecule (see Figures 1 and 2). The cleavage of the tetrahedral intermediate is strongly exergonic, the calculated reaction energy being -47.7 and -62.5 and -65.9 kcal mol^{-1} for the **P(AZ)**, **P(FAZ)-*syn***, and **P(FAZ)-*anti*** conformers, respectively.

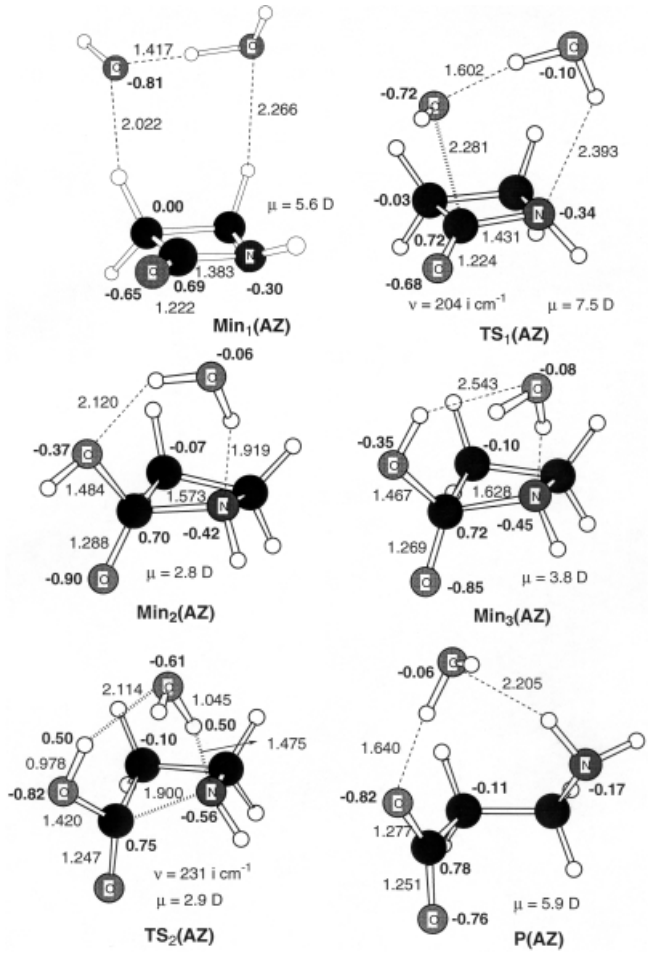

Figure 1. B3LYP/6-31+G* optimized structures for the water-assisted alkaline hydrolysis of 2-azetidinone (**AZ**). Distances in Å. B3LYP/6-31+G* NPA atomic charges in bold characters (H atoms summed into heavy atoms to which they are bonded).

When comparing these processes, we see that the presence of the 3-formylamino side chain causes an important stabilization all along the reaction coordinate (see Tables 1–2) owing to its electron-withdrawing ability, clearly manifested when comparing the NPA charges of C3 in the structures in Figures 1 and 2. As mentioned above, this stabilization also stems from the ability of the amino group of this side chain to interact via a hydrogen bond with the hydroxyl moiety along the *syn* attack or with the β-lactam carbonyl oxygen atom along the *anti* attack (see Figure 2). Overall, the 3-formylamino side chain considerably facilitates both the attack of the hydroxyl ion and the electron density rearrangement necessary for the β-lactam C–N bond cleavage in the gas phase. In addition, the 3-formylamino group has an important thermodynamic effect by stabilizing around 14–19 kcal mol^{-1} the negatively charged carboxylate group at the product complex **P(FAZ)**.

Hydrolysis of the 3-formylamino-2-azetidine-1-sulfonate ion: Our calculations rendered a new mechanism for the hydrolysis of the 3-formylamino-2-azetidine-1-sulfonate ion in which the SO_3 group plays an active role by assisting the proton transfer events along the reaction coordinate. Figure 3 shows the critical structures located on the B3LYP/6-31+G* PES and Table 3 gives the corresponding relative energies. In the gas phase, this process proceeds through substantially higher barriers than in the two previous cases because both reactants have now a negative charge.

In the reactant complex **Min$_1$(FAZS)-*syn***, the hydroxyl ion strongly interacts with the 3-formylamino side chain through a NH$\cdots$O hydrogen bond of $\approx$1.5 Å. This complex results quite similar to that found in the *syn* route for the hydrolysis of **FAZ** (**Min$_1$(FAZ)-*syn***). For the *anti* approach of the $OH^-\cdots(H_2O)$ dimer towards the carbonyl group of **FAZS**, a representative precursor complex could not be located on the B3LYP/6-31+G* PES.

TS$_1$(FAZS)-*syn* and **TS$_1$(FAZS)-*anti*** are the transition structures corresponding to the addition of OH^- to the monobactam and present energy barriers of 43.2 and 51.3 kcal mol^{-1}, respectively. The energy difference between both TSs (8.1 kcal mol^{-1}) can be ascribed to the short hydrogen-bond interaction between the hydroxyl anion and the hydrogen atom bonded to the formylamino side chain in the *syn* approach (N-H$\cdots$O 1.891 Å, see Figure 3). This interaction allows a closer approach of the nucleophile rendering a more advanced TS for the *syn* attack. The addition products obtained from these TSs are **Min$_2$(FAZS)-*syn*** and **Min$_2$-(FAZS)-*anti*** which are 42.6 and 40.6 kcal mol^{-1}, respectively above separate reactants and correspond to tetrahedral intermediates. In these structures, the ancillary water molecule bridges the hydroxyl and the SO_3 groups by means of two hydrogen bonds with equilibrium distances of $\approx$1.9 Å.

We found that the most favorable route for the evolution of the addition tetrahedral species takes place through the conformers **Min$_3$(FAZS)-*syn*** and **Min$_3$(FAZS)-*anti*** in which the ancillary water molecule bridges the forming carboxylate group with the SO_3 group. **Min$_3$(FAZS)-*syn*** and **Min$_3$(FAZS)-*anti*** are 2.0 and 3.2 kcal mol^{-1}, respectively, more stable than the addition intermediates **Min$_2$(FAZS)-*syn*** and **Min$_2$-(FAZS)-*anti***. According to our calculations, **Min$_3$(FAZS)-*syn*** and **Min$_3$(FAZS)-*anti*** are connected along the reaction coordinate with **TS$_2$(FAZS)-*syn*** and **TS$_2$(FAZS)-*anti***, respectively, which are transition states for the ring opening and double proton transfer from the OH group to water and from water to the SO_3 moiety. Energetically, **TS$_2$(FAZS)-*syn*** is 4.1 kcal mol^{-1} above **Min$_3$(FAZS)-*syn***, while **TS$_2$(FAZS)-*anti*** is 5.1 kcal mol^{-1} above **Min$_3$(FAZS)-*anti***. These TS structures lead to **Min$_4$(FAZS)-*syn*** and **Min$_4$(FAZS)-*anti*** in which the β-lactam ring is already open. Thus, owing to the release of the β-lactam strain energy, **Min$_4$(FAZS)-*syn*** and **Min$_4$(FAZS)-*anti*** are about 20 kcal mol^{-1} more stable than their precursors. In the intermediates **Min$_4$(FAZS)-*syn*** and **Min$_4$(FAZS)-*anti***,

0947-6539/02/0804-0862 $ 17.50+.50/0 *Chem. Eur. J.* **2002**, *8*, No. 4

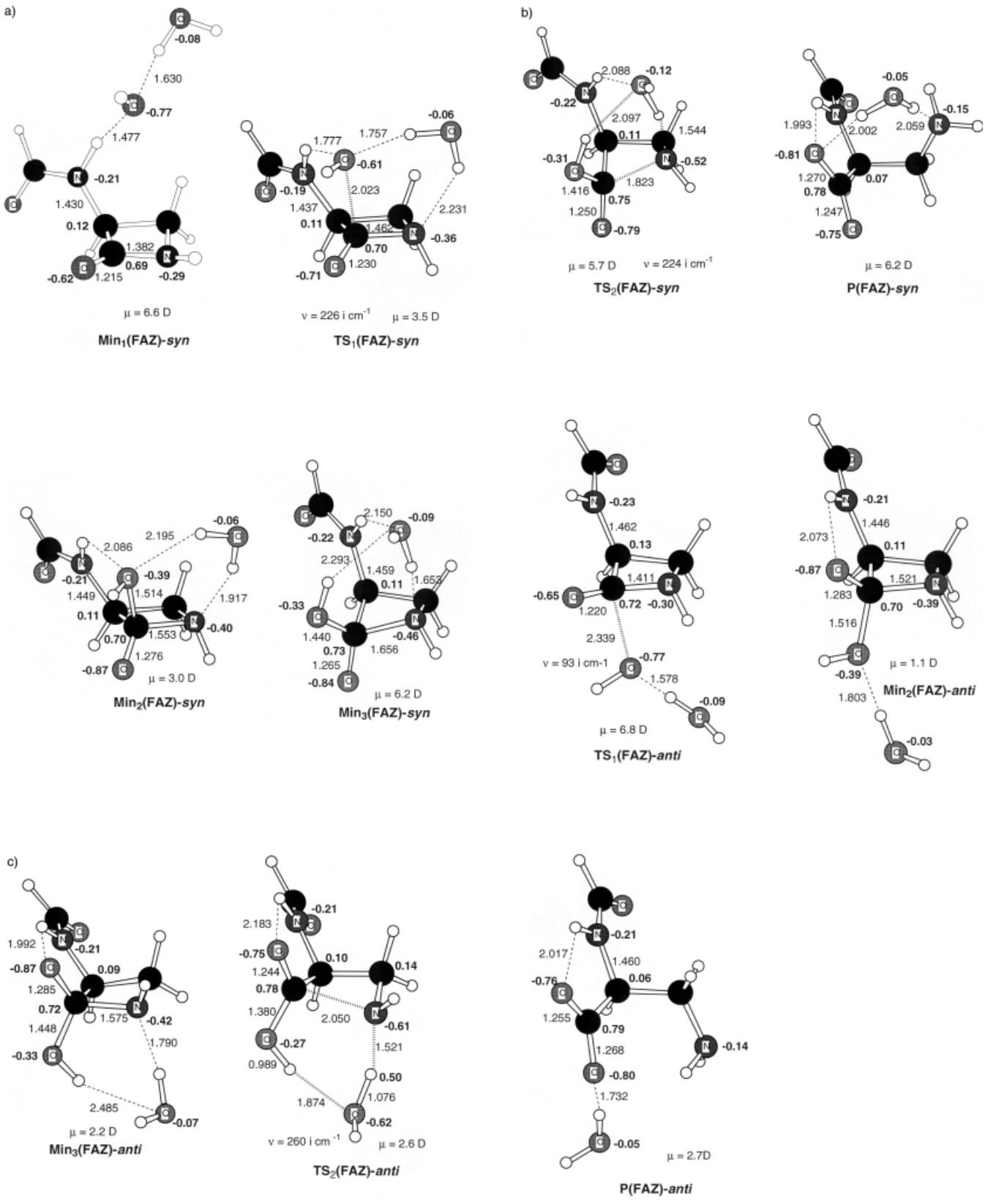

Figure 2. B3LYP/6-31+G* optimized structures for the water-assisted alkaline hydrolysis of 3-formylamino-2-azetidinone (**FAZ**). Critical structures are shown for both the *syn* and *anti* approaches of the nucleophile with respect to the formylamino side chain of the β-lactam. Distances in Å. B3LYP/6-31+G* NPA atomic charges in bold characters (H atoms summed into heavy atoms to which they are bonded).

Table 1. Relative energies [kcal mol^{-1}] for the H_2O-assisted alkaline hydrolysis of 2-azetidinone.

	B3LYP/6-31+G*[a]	$\Delta G_{\text{gas phase}}$	$\Delta\Delta G_{\text{solvation}}$	$\Delta G_{\text{solution}}$
2-azetidinone $+OH^-\cdots(H_2O)$	0.0	0.0	0.0	0.0
Min_1(AZ)	−14.3	−4.9	25.7	20.8
TS_1(AZ)	−0.7	10.5	10.6	21.1
Min_2(AZ)	−10.4	1.4	18.4	19.7
Min_3(AZ)	−5.2	6.0	14.7	20.7
TS_2(AZ)	−4.8	7.2	19.3	26.5
P(AZ)	−47.7	−36.9	19.6	−17.3

[a] Including B3LYP/6-31+G* ZPVE.

Table 2. Relative energies [kcal mol^{-1}] for the H_2O-assisted alkaline hydrolysis of the 3-formylamino-2-azetidinone.

	B3LYP/6-31+G*[a]	$\Delta G_{\text{gas phase}}$	$\Delta\Delta G_{\text{solvation}}$	$\Delta G_{\text{solution}}$
3-formylamino-2-azetidinone $+OH^-\cdots(H_2O)$	0.0	0.0	0.0	0.0
Min_1(FAZ)-*syn*	−35.0	−25.8	36.5	10.7
TS_1(FAZ)-*syn*	−19.8	−7.5	31.6	24.1
Min_2(FAZ)-*syn*	−23.4	−11.8	27.8	16.0
Min_3(FAZ)-*syn*	−14.9	−2.5	22.6	20.2
TS_2(FAZ)-*syn*	−15.5	−2.6	27.2	24.6
P(FAZ)-*syn*	−62.5	−51.0	30.4	−20.6
Min_1(FAZ)-*anti*	−10.6	−0.7	22.0	21.3
TS_1(FAZ)-*anti*	−14.8	−4.8	23.0	18.1
Min_2(FAZ)-*anti*	−20.9	−10.9	25.4	14.5
Min_3(FAZ)-*anti*	−22.4	−10.9	26.8	16.0
TS_2(FAZ)-*anti*	−18.8	−6.2	31.6	25.4
P(FAZ)-*anti*	−65.9	−56.1	34.0	−22.0

[a] Including B3LYP/6-31+G* ZPVE.

Table 3. Relative energies [kcal mol^{-1}] for the H_2O-assisted alkaline hydrolysis of the 3-formylamino-2-azetidine-1-sulfonate ion.

	B3LYP/6-31+G*[a]	$\Delta G_{\text{gas phase}}$	$\Delta\Delta G_{\text{solvation}}$	$\Delta G_{\text{solution}}$
3-formylamino-2-azetidine-1-sulfonate$+OH^-\cdots(H_2O)$	0.0	0.0	0.0	0.0
Min_1(FAZS)-*syn*	17.2	26.5	−19.6	6.9
TS_1(FAZS)-*syn*	43.2	56.6	−34.9	21.8
Min_2(FAZS)-*syn*	42.6	56.1	−37.4	18.6
Min_3(FAZS)-*syn*	40.6	54.6	−37.4	17.2
TS_2(FAZS)-*syn*	44.7	58.8	−40.7	18.1
Min_4(FAZS)-*syn*	20.6	33.6	−32.5	1.1
TS_3(FAZS)-*syn*	24.0	37.4	−27.7	9.7
P(FAZS)-*syn*	−7.0	5.1	−27.6	−22.4
Min_1(FAZS)-*anti*	40.9	45.7	−29.7	16.0
TS_1(FAZS)-*anti*	51.3	64.9	−33.0	32.0
Min_2(FAZS)-*anti*	40.6	54.2	−37.1	17.1
Min_3(FAZS)-anti	37.4	50.8	−34.6	16.2
TS_2(FAZS)-*anti*	42.5	56.7	−39.2	17.6
Min_4(FAZS)-*anti*	17.1	30.1	−30.5	−0.4
TS_3(FAZS)-*anti*	24.0	37.1	−29.9	7.2
P(FAZS)-*anti*	−8.6	3.4	−29.2	−25.7

[a] Including B3LYP/6-31+G* ZPVE.

the location of the catalytic water molecule, which is interacting with the SO_3H moiety, the nitrogen atom, and one of the oxygen atoms of the carboxylate group (see Figure 3), is clearly adequate for assisting the $N-SO_3H \rightarrow NH-SO_3$ proton transfer. We found that this process takes place with the assistance of the water molecule through **TS_3(FAZS)-*syn*** and **TS_3(FAZS)-*anti*** to yield the product conformers of the hydrolysis reaction, **P(FAZS)-*syn*** and **P(FAZS)-*anti***. The energy barrier for this step amounts to 3-7 kcal mol^{-1} with respect to the **Min_4(FAZS)** structures.

As this is a dianionic system we have investigated whether the wave function is bound with respect to vertical loss of one electron for all structures along the reaction pathways. In all the cases this condition was satisfied.

Gibbs energy profiles in the gas phase and in solution: The relative B3LYP/6-31+G* Gibbs energy values with respect to the $OH^-\cdots(H_2O)$ complex and the corresponding β-lactam compound are given in Tables 1–3 for the hydrolysis of 2-azetidinone, 3-formylamino-2-azetidinone, and 3-formylamino-2-azetidine-1-sulfonate ion, respectively, both in the gas phase and in solution. Figures 4 and 5 display the Gibbs energy profiles for the three processes in solution.

When thermal corrections to the B3LYP/6-31+G* gas phase 0 K energies are included, a destabilization of the energy profiles with respect to the separate reactants takes place in the three cases owing to the entropy factor. For 2-azetidinone and 3-formylamino-2-azetidinone, this destabilization amounts to about 10–13 kcal mol^{-1} and for the 3-formylamino-2-azetidine-1-sulfonate ion to about 12–14 kcal mol^{-1}. All the prereactive complexes can be only transient species when the thermal corrections and solvation energies are included (see Tables 1–3).

Owing to the strong polarization of the continuum by the $OH^-\cdots(H_2O)$ complex, the electrostatic effect of solvent stabilizes preferentially the separate reactants over the remaining critical structures along the reaction coordinate by around 10–20 kcal mol^{-1} for 2-azetidinone and 23–34 kcal mol^{-1} for 3-formylamino-2-azetidinone. The greater effect in the latter case originates from the previously discussed electron withdrawing effect of the 3-formylamino side chain which avoids the concentration of negative charge thus weakening the electrostatic solute–solvent interaction.

On the contrary, for the 3-formylamino-2-azetidine-1-sulfonate ion, the whole energy profile becomes more stabilized in solution than separate reactants by around 28–41 kcal mol^{-1} because solute–solvent interactions largely overcome the electrostatic repulsion between the negatively charged reactants. Most interestingly, the sulfonate group plays an important role by accumulating a large negative charge ($\approx$1.4 e$^-$) that is developed at the critical structures involved in the breakdown of the tetrahedral intermediates and strongly polarizing the solvent. In this way, the energy barrier in solution relative to reactants corresponding to the C–N bond cleavage considerably diminishes with respect to those of the **AZ** and **FAZ** systems, and therefore the ring of the monobactam is readily and irreversibly opened after the initial addition of the hydroxyl anion. The influence of the SO_3 group to facilitate the rupture of the endocylic C–N bond is also in agreement with the poor basic character of the leaving amino group.

As a result of both entropic and solvent effects, for 2-azetidinone the rate determining step corresponds to the opening of the β-lactam ring with a Gibbs energy barrier in solution of 26.5 kcal mol^{-1}. In the case of 3-formylamino-2-azetidinone, the most favorable route is the *syn* one, in which a rate determining step is the β-lactam ring cleavage with a

0947-6539/02/0804-0864 $ 17.50+.50/0 *Chem. Eur. J.* **2002**, *8*, No. 4

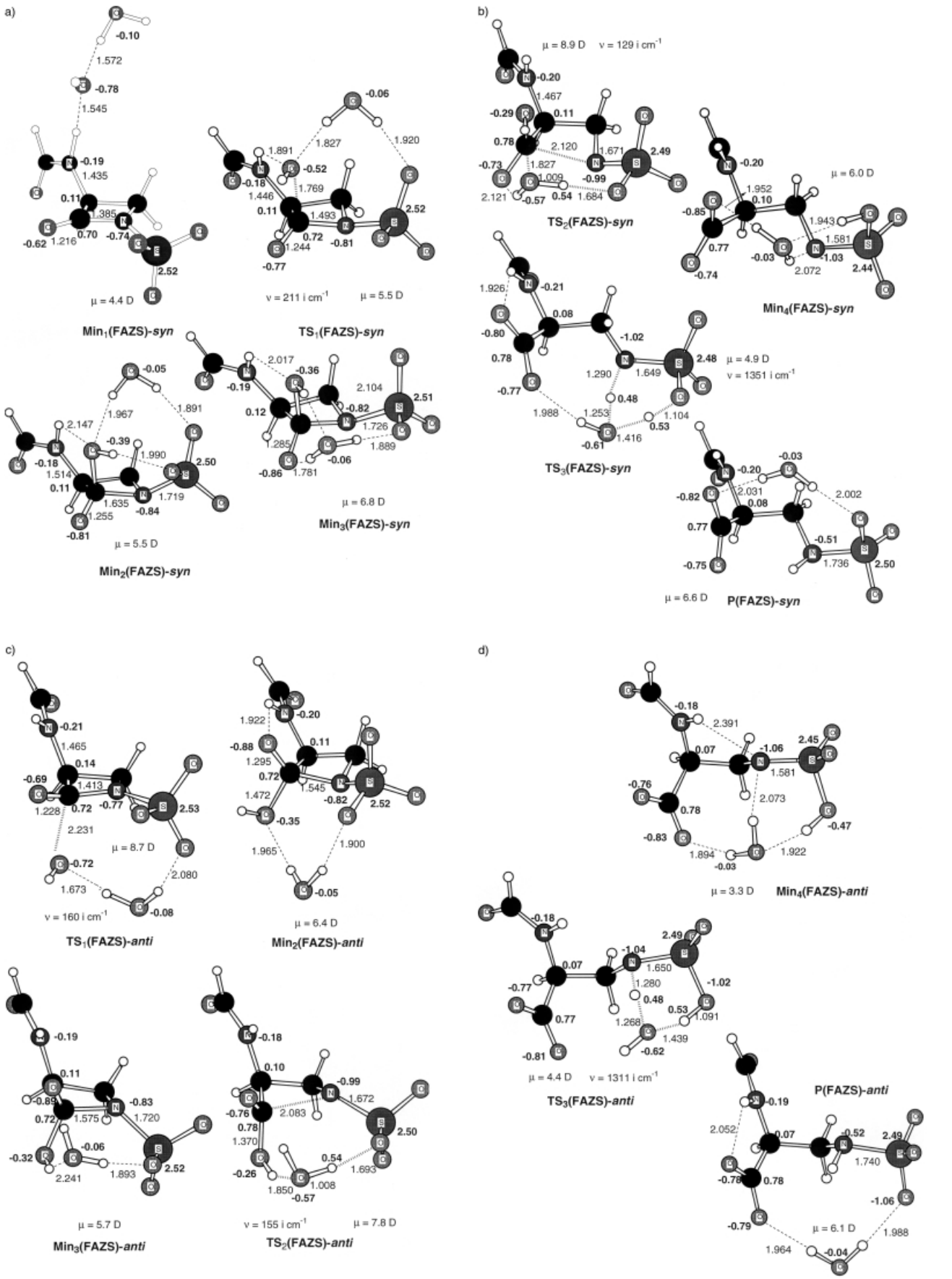

Figure 3. B3LYP/6-31+G* optimized structures for the water-assisted alkaline hydrolysis of the 3-formylamino-2-azetidine-1-sulfonate ion (**FAZS**). Critical structures are shown for both the *syn* and *anti* approaches of the nucleophile with respect to the formylamino side chain of the β-lactam. Distances in Å. B3LYP/6-31+G* NPA atomic charges in bold characters (H atoms summed into heavy atoms to which they are bonded).

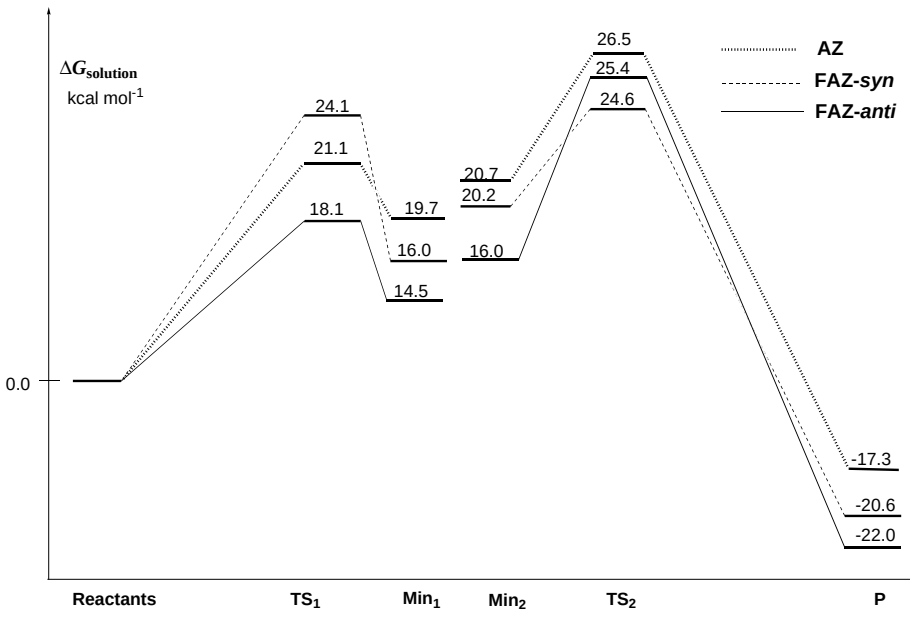

Figure 4. Gibbs energy profiles [kcal mol^{-1}] in solution for the hydrolysis reaction of 2-azetidinone (**AZ**) and 3-formylamino-2-azetidinone (**FAZ**).

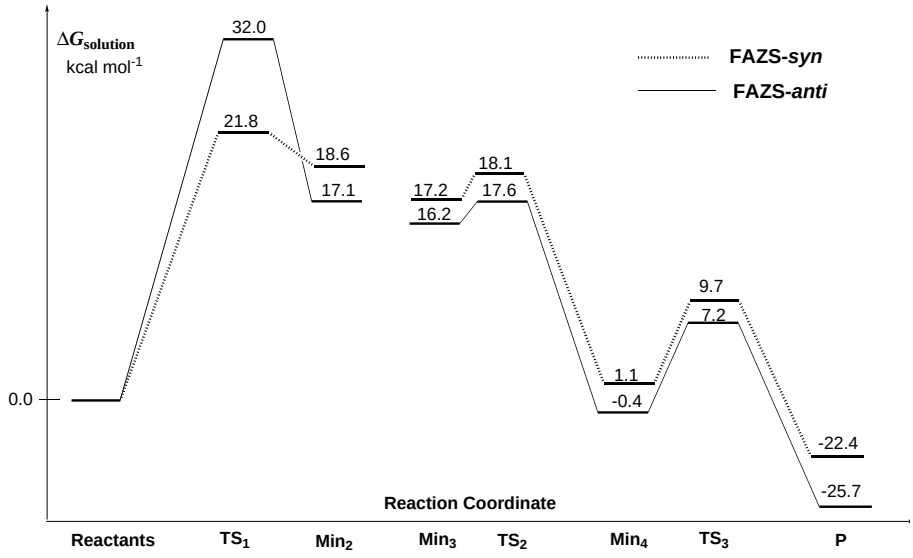

Figure 5. Gibbs energy profiles [kcal mol^{-1}] in solution for the hydrolysis reaction of the 3-formylamino-2-azetidine-1-sulfonate ion (**FAZS**).

Gibbs energy barrier of 24.6 kcal mol^{-1} (only 0.8 kcal mol^{-1} more stable in solution than the corresponding *anti* structure). For 3-formylamino-2-azetidine-1-sulfonate ion, the *syn* process is 10.2 kcal mol^{-1} more favorable than the *anti* process and the rate determining step now corresponds to the nucleophilic attack of the hydroxyl anion with a Gibbs energy barrier of 21.8 kcal mol^{-1}.

Comparison with experiment: Let us now compare our results in solution with experiment. The theoretical $\Delta G^{\neq}$ values obtained in solution, 26.5 and 24.6 kcal mol^{-1} for 2-azetidinone and 3-formylamino-2-azetidinone (*syn*), respectively, agree reasonable well with the range of experimental values (18.2 – 25.4 kcal mol^{-1}) previously reported[12b] for *N*-methyl-, *N*-phenyl-β-lactams, and penicillins.

The $\Delta G_{solution}$ calculations on the 2-azetidinone and 3-formylamino-2-azetidinone systems, yield for the kinetic effect of the 3-formylamino side chain 1.9 kcal mol^{-1} at the TS for the opening of the β-lactam ring in agreement with the experimental estimation reported (2.1 kcal mol^{-1}).[12b] As mentioned previously, this effect originates from the electron-withdrawing and hydrogen-bonding ability of the formylamino group which allows for less repulsive electrostatic interactions when the β-lactam is approached by the hydroxide anion and an easier electron rearrangement when the β-lactam ring opens.

For the hydrolysis of the 3-formylamino-2-azetidine-1-sulfonate ion, the calculated rate-determining barrier $\Delta G_{solution}$ for the *syn* profile (21.8 kcal mol^{-1}) which corresponds to a kinetic constant[32] of $k = 47.9 \times 10^{-1}$ mol^{-1} dm^3 h^{-1}, is in agreement with the experimental data reported for the alkaline hydrolysis of aztreonam at 35 °C (experimental activation energy = 22.4 kcal mol^{-1}; $k = 2.12 \times 10^{-1}$ mol^{-1} dm^3 h^{-1}).[13] On the other hand, it is an experimental fact that monobactam antibiotics have a similar reactivity than benzylpenicillin toward alkaline hydrolysis.[14] To further address this point, we also investigated the nucleophilic attack of the hydroxyl anion to 6-formylamino-3α-carboxypenam (a model of penicillin compounds, see also the Supporting Information). The calculated $\Delta G_{solution}$ value for the penicllin model amounts to 19.9 kcal mol^{-1} which, in effect, turns out to be close to that of the monobactam model.

The 3-formylamino-2-azetidine-1-sulfonate ion has a good leaving group because of the effect of the SO_3 substituent. For this system our calculations clearly render as the rate determining step the first one corresponding to the addition of the hydroxide ion.[32] This result is in agreement with the experimental Brønsted β values which are indicative of rate-limiting nucleophilic attack for the hydrolysis of β-lactam antibiotics including monobactams.[11, 15] Comparison between the energy profiles shown in Figures 4 and 5 supports clearly the proposal[14, 15] that β-lactams of the more basic amines (i.e., 2-azetidinone and 3-formylamino-2-azetidinone) present a larger energy barrier for the breakdown of the β-lactam C–N bond with respect to β-lactams with good leaving groups (i.e., 3-formylamino-2-azetidine-1-sulfonate).

0947-6539/02/0804-0866 $ 17.50+.50/0 *Chem. Eur. J.* **2002**, *8*, No. 4

Conclusion

The theoretical results obtained in the present work reproduce quite reasonably the basic experimental facts and give insight into the molecular details of the reaction mechanism for the alkaline hydrolysis of β-lactams. According to our calculations, the rate determining step for the alkaline hydrolysis of the 3-formylamino-2-azetidine-1-sulfonate ion is the nucleophilic attack on the carbonyl carbon atom. The most favored pathway for the hydroxyl addition takes place in a *syn* orientation with respect to the 3-formylamino side chain. The kinetic effect of the formylamino side chain stems from both its electron-withdrawing and hydrogen-bonding abilities. The SO_3 group facilitates the opening of the β-lactam ring by making the nitrogen atom less basic and by enhancing the solute–solvent interactions. Our calculations also indicate that the SO_3 group plays an active role by favoring the proton transfer to the leaving amino group through a $N{-}SO_3H \rightarrow NH{-}SO_3$ isomerization assisted by the ancillary water molecule. Globally, the Gibbs energy profiles and the molecular knowledge gained in this work may be helpful to further understand the similarities and differences in the biochemical activity of monobactams and bicyclic β-lactam antibiotics.

Acknowledgements

We thank MEC (Spain) for financial support (PB97-1300 and PB96-0795). N.D. also thanks MEC for her grant PB98-44430549. We are also grateful to one of the referees for his/her interesting comments and suggestions.

[1] *The Chemistry of β-Lactams* (Ed.: M. I. Page), Blackie Academic, London, **1992**.
[2] M. I. Page, *Chem. Commun.* **1998**, 1609–1617.
[3] S. G. Waley, *β-lactamase*: *Mechanism of action* in *The Chemistry of β-Lactams* (Ed.: M. I. Page), Blackie Academic, London, **1992**, pp. 199–228.
[4] Z. Wang, W. Fast, A. M. Valentine, S. J. Benkovic, *Curr. Opin. Chem. Biol.* **1999**, *3*, 614–622.
[5] A. Imada, K. Kitano, K. Kintaka, M. Muroi, M. Asai, *Nature* **1981**, *289*, 590–591.
[6] R. B. Sykes, C. M. Cimarusti, D. P. Bonner, K. Bush, D. M. Floyd, N. H. Georgopapadakou, W. H. Koster, W. C. Liu, W. L. Parker, P. A. Principe, M. L. Rathnum, W. A. Slusarchyk, W. H. Trejo, J. S. Wells, *Nature* **1981**, *291*, 489–491.
[7] C. M. Cimarusti, R. B. Sykes, *Chem. Br.* **1983**, 302–303.
[8] W. C. Hellinger, N. S. Brewer, *Mayo Clin. Proc.* **1999**, *74*, 420–434.
[9] K. Bush, *Clin. Infect. Dis.* **1998**, *27* (Suppl. 1), S48–S53.
[10] I. Heinze-Krauss, P. Angehrn, R. L. Charnas, K. Gubernator, E. M. Gutknecht, C. Huschwerlen, M. Kania, C. Oefner, M. C. P. Page, S. Sogabe, J. L. Specklin, F. Winkler, *J. Med. Chem.* **1998**, *41*, 3961–3971.
[11] M. I. Page, *Structure-Activity Relationships*: *Chemical* in *The Chemistry of β-Lactams* (Ed.: M. I. Page), Blackie Academic, London, **1992**, pp. 79–100.
[12] a) K. Bowden, K. Bromley, *J. Chem. Soc. Perkin Trans. 2* **1990**, 2111–2116; b) K. Bowden, K. Bromley, *J. Chem. Soc. Perkin Trans. 2* **1990**, 2103–2109.
[13] R. Menéndez, T. Alemany, J. Martín-Villacorta, *Chem. Pharm. Bull.* **1992**, *40*, 3222–3227.
[14] M. I. Page, *Acc. Chem. Res.* **1984**, *17*, 144–151.
[15] P. Proctor, N. P. Gensmantel, M. I. Page, *J. Chem. Soc. Perkin Trans. 2* **1982**, 1185–1192.
[16] I. Massova, P. A. Kollman, *J. Phys. Chem. B.* **1999**, *10*, 8628–8638, and references therein.
[17] a) D. B. Boyd, R. B. Hermann, D. E. Presti, M. M. Marsh, *J. Med. Chem.* **1975**, *18*, 408–417; b) D. B. Boyd, in *Chemistry and Biology of β-Lactam Antibiotics* (Ed.: R. B. Morin, M. Gorman), Academic Press, New York, **1982**.
[18] a) C. Petrongolo, G. Ranghino, R. Scordamaglia, *Chem. Phys.* **1980**, *45*, 279–290; b) C. Petrongolo, E. Pescatori, G. Ranghino, R. Scordamaglia, *Chem. Phys.* **1980**, *45*, 291–304; c) C. Petrongolo, G. Ranghino, *Theor. Chim. Acta* **1980**, *54*, 239–243.
[19] a) J. Frau, J. Donoso, F. Muñoz, F. García-Blanco, *J. Comput. Chem.* **1992**, *13*, 681–692; b) J. Frau, J. Donoso, B. Vilanova, F. Muñoz, F. García-Blanco, *Theor. Chim. Acta* **1993**, *86*, 229–239; c) J. Frau, J. Donoso, F. Muñoz, F. García-Blanco, *Helv. Chim. Acta* **1996**, *79*, 353–362; d) J. Frau, J. Donoso, F Muñoz, B. Vilanova, F. García Blanco, *Helv. Chim. Acta* **1997**, *80*, 739–747; e) J. Frau, J. Donoso, F. Muñoz, B. Vilanova, F. García Blanco, *J. Mol. Struct. (Theochem)* **1998**, *426*, 313–321.
[20] Y. G. Smeyers, A. Hernández-Laguna, R. González-Jonte, *J. Mol. Struct. (Theochem)* **1993**, *106*, 261–268.
[21] S. Wolfe, C. K. Kim, K. Yang, *Can. J. Chem.* **1994**, *72*, 1033–1043.
[22] a) J. Pitarch, M. F. Ruiz-López, J. L. Pascual-Ahuir, E. Silla, I. Tuñón, *J. Phys. Chem.* **1997**, *101*, 3581–3588; b) J. Pitarch, M. F. Ruiz-López, E. Silla, J. L. Pascual-Ahuir, I. Tuñón, *J. Am. Chem. Soc.* **1998**, *120*, 2146–2155.
[23] a) J. Pitarch, J. L. Pascual-Ahuir, E. Silla, I Tuñón, M. F. Ruiz-López, *J. Comput. Chem.* **1999**, *20*, 1401–1411; b) J. Pitarch, J. L. Pascual-Ahuir, E. Silla, I Tuñón, M. F. Ruiz-López, C. Millot, J. Bertrán, *Theor. Chem. Acc.* **1999**, *101*, 336–342.
[24] J. A. Sowek, S. B. Singer, S. Ohringer, M. F. Malley, T. J. Dougherty, J. Z. Gougoutas, K. Bush, *Biochemistry* **1991**, *30*, 3179–3188.
[25] *Gaussian 98*, Revision A. 6, M. J. Frisch, G. W. Trucks, H. B. Schlegel, G.E Scuseria, M. A. Robb, J. R. Cheeseman, V. G. Zakrzewski, J. A. Montgomery, R. E. Stratmann, Jr., J. C. Burant, S. Dapprich, J. M. Millam, A. D. Daniels, K. N. Kudin, M. C. Strain, O. Farkas, J. Tomasi, V. Barone, M. Cossi, R. Cammi, B. Mennucci, C. Pomelli, C. Adamo, S. Clifford, J. Ochterski, G. A. Petersson, P. Y. Ayala, Q. Cui, K. Morokuma, D. K. Malick, A. D. Rabuck, K. Raghavachari, J. B. Foresman, J. Cioslowski, J. V. Ortiz, B. B. Stefanov, G. Liu, A. Liashenko, P. Piskorz, I. Komaromi, R. Gomperts, R. L. Martin, D. J. Fox, T. Keith, M. A. Al-Laham, C. Y. Peng, A. Nanayakkara, C. Gonzalez, M. Challacombe, P. M. W. Gill, B. Johnson, W. Chen, M. W. Wong, J. L. Andres, C. Gonzalez, M. Head-Gordon, E. S. Replogle, J. A. Pople, Gaussian, Inc., Pittsburgh PA, **1998**.
[26] D. A. McQuarrie, *Statistical Mechanics*, Harper & Row, New York, **1986**.
[27] a) J. L. Rivail, D. Rinaldi, M. F. Ruiz-López, in *Theoretical and Computational Model for Organic Chemistry*, *Vol. 339* (Eds.: S. J. Formosinho, I. G. Csizmadia, L. Arnaut), NATO ASI Series C, Kluwer, Dordrecht, **1991**, p. 79–92; b) J. Tomasi, M. Persico, *Chem. Rev.* **1994**, *94*, 2027–2094; c) J. Tomasi, R. Cammi, *J. Comput. Chem.* **1995**, *16*, 1449–1458; d) C. J. Cramer, D. G. Truhlar, *Chem. Rev.* **1999**, *99*, 2161–2193.
[28] a) J. L. Pascual-Ahuir, E. Silla, J. Tomasi, R. Bonaccorsi, *J. Comput. Chem.* **1987**, *8*, 778–784; b) J.L Pascual-Ahuir, E. Silla, I. Tuñón, *J. Comput. Chem.* **1994**, *15*, 1127–1138.
[29] V. Barone, M. Cossi, J. Tomasi, *J. Chem. Phys.* **1997**, *107*, 3210–3221.
[30] In order to further validate the solvation model used we have calculated the solvation free energies of some small ions: OH^-, CH_3O^-, CH_3COO^-, and HS^-. The $\Delta G_{solvation}$ calculated with the PCM-UAHF model are, respectively, -104.5, -88.6, -74.7, and -71.5 kcal mol^{-1} compared with the experimental values of -110.0, -98.0, -77.0, and -76.0 kcal mol^{-1}. These results show that the PCM-UAHF model gives reasonable values justifying its use in our work.
[31] A. E. Reed, R. B. Weinstock, F. Weinhold, *J. Chem. Phys.* **1985**, *83*, 735–746.
[32] The estimated k value is obtained using the conventional transition state theory.

Received: October 11, 2000
Revised: August 2, 2001 [F2791]